BIOTITES INTERMEDIATE BETWEEN DIOCTAHEDRAL AND TRIOCTAHEDRAL MICAS

by

J. RIMSAITE

Geological Survey of Canada, Ottawa, Canada

ABSTRACT

ORANGE-YELLOW detrital flakes of biotite are common carriers of potassium and trace elements in soils and clays. Because the flakes differ in degree of alteration and may be derived from different sources, it is difficult to obtain homogeneous material for studies of their physical and chemical properties that may be compared with the original mica. A similar orange-yellow altered biotite occurs with fresh biotites in alkalic rocks of a nepheline deposit. The fresh and altered biotites were separated for chemical and mineralogical studies of the effects of weathering on biotite in its parent rock.

The common iron-rich biotites with octahedral occupancy between 5.5 and 5.8 alter to bright orange-yellow biotites with octahedral occupancy approaching five. These biotites, intermediate between the trioctahedral and dioctahedral micas, form as a result of oxidation during the process of their alteration to chlorite–vermiculite.

Biotites with octahedral occupancy approaching five were prepared experimentally by heating a natural biotite that contained high ferrous iron. The main differences between the natural and laboratory oxidized biotites are: the naturally oxidized micas lose 30% of the original potassium, adsorb about 2 wt.% water, and apparently gain about 25% hydroxyl, whereas laboratory oxidized micas retain potassium and lose hydroxyl and argon. The oxidized micas retain the crystal structure of the original mica.

INTRODUCTION

DETRITAL minerals constitute a considerable proportion of soils and clays. Micas are of particular importance because on disintegration they supply potassium, magnesium, iron, and trace elements. Processes of weathering of micas and changes of physical and chemical properties of fresh and weathered mica-bearing rocks have therefore been studied by numerous mineralogists and chemists. Goldschmidt and Johnson (1922) studied the distribution of potassium in fresh and altered minerals in soils of Northern temperate regions and concluded that iron-rich biotite supplies more potassium to the soil than potassium feldspar. Eskola (1936) discussed several causes of crumbling of Finnish rapakivi granite and pointed out an apparent relationship between the degree of disintegration of granite and its lepidomelane content. He compared chemical analyses of fresh biotite from compact

https://doi.org/10.1346/CCMN.1967.0150139 Published online by Cambridge University Press

rock and of orange-yellow altered biotite from crumbling rock and demonstrated significant changes in oxidation of iron, hydration, and loss of potassium in the altered biotite (Eskola, 1949, p. 114). Walker (1949) studied decomposition of biotite in soil and distinguished several stages of weathering. Grant (1964) described chemical weathering of biotite plagioclase gneiss and discussed changes in some physical properties of the biotite.

The writer calculated structural formulae of weathered biotites from analyses published by Eskola (1949) and Walker (1949) and observed that the octahedral occupancy of these oxidized biotites is 5.14 and 4.6, which is between that of the dioctahedral and the trioctahedral micas. The occurrence of such intermediate micas led the writer to make a more detailed study of the chemical, physical, and structural properties of natural and laboratory oxidized biotites.

The purposes of this article are (1) to describe physical, chemical, and structural properties of the original trioctahedral biotites and their hydrous and dehydrated alteration products, and (2) to discuss the differences between ideal dioctahedral and trioctahedral micas and biotites with intermediate octahedral occupancy.

SAMPLES AND PROCEDURES

In the Blue Mountain area of Ontario, orange-yellow biotite occurs as an alteration product of iron-rich biotites in nepheline syenite pegmatite, biotite schist, gneissic nepheline syenite and in paragneiss. The following biotites were collected in the Blue Mountain area and separated in the laboratory.

43F: Brown fresh biotite from mica-rich xenolith. The biotite has a few fine-grained inclusions along the edges.

44F: Green, fresh, coarse-grained pegmatitic biotite, relatively compact.

44W: Orange-yellow biotite, a weathering product of biotite *44F*. The orange biotite is split along (001) cleavage planes and has small polygonal fractures on the surface. Biotite *44W* forms coatings on the surface and along the cleavage planes and fractures of the green biotite *44F*. Biotites *44F* and *44W* were concentrated from a single crystal.

44FC and *44WC:* fresh and weathered biotites heated 20 hr in air at 650°C. The time required to reach 650°C was approximately 2 hr.

45F: Mainly green, coarse pegmatitic biotite, similar to *44F*, altered to orange-yellow biotite along the fractures. In addition, the concentrate *45F* contains about 5% of fine-grained green biotite and about 5% of brown flakes resembling those of biotite *43F*.

45W: Orange-yellow alteration crusts of biotite *45F*, similar to *44W*. The altered biotite is split along (001) cleavage planes and has polygonal fractures on the surface. About 10% of the orange flakes are interleaved with green and brown biotite.

46F: Fresh, brown and olive-green biotite from paragneiss.

46W: Orange-yellow alteration product of biotite *46F*. The altered biotite has a speckled surface and it is split along the (001) cleavage planes.

https://doi.org/10.1346/CCMN.1967.0150139 Published online by Cambridge University Press

46FC and *46WC:* the fresh and weathered biotites heated in air 20 hr at 620°C. The time required to reach 620°C was approximately 2 hr.

Specimens from other localities included:

31 green: fresh, green pegmatitic biotite from the Bancroft area, Ontario. The biotite was previously studied in detail by the writer (Rimsaite, 1964). It alters along fractures to orange-yellow biotite *31 orange*. The yellow biotite has polygonal fractures on the surface, illustrated by the writer in a previous report (Rimsaite, 1963, pl. III-5). Fresh and weathered portions of biotite *31* are similar in appearance to those of biotites *44* and *45*.

27: Biotite from cordierite schist, District of Mackenzie, was used for laboratory experiments of oxidation and dehydration, and for studies of retention of radiogenic argon in the dehydrated and oxidized samples. The chemical analysis of biotite *27* was published previously (Rimsaite, 1964).

27A: Biotite *27* heated in air 20 hr at 450°C. The time required to reach 450°C was 1 hr. The heated biotite is heterogeneous. Greenish and brownish flakes are discoloured orange-yellow along fractures and edges.

27B: Biotite *27* heated in argon 20 hr at 650°C (argon pressure = 1 atm). The heating rate before reaching 650°C was 12°C per min. The heated biotite is composed of heterogeneous flakes that vary in colour from bright orange-red to dull brown and opaque.

27C: Biotite *27* heated in air 20 hr and 500 hr at 650°C (*27C* heated 500 hr was used for isotopic studies). The heating rate before reaching 650°C was 6°C per min. The heated samples are bright orange-red.

27D: Biotite *27* heated in vacuum 20 hr at 650°C. (Reduced pressure = 0.1 mm Hg.) The heating rate before reaching 650°C was 12°C per min. The flakes of heated biotite vary in colour from bright orange-red to pale orange. All heated flakes are split along (001) cleavage planes, blistered and very brittle.

All micas were concentrated in heavy liquids and by means of a Frantz Isodynamic Separator. The separation procedure was time-consuming because the specific gravities and magnetic susceptibilities of fresh and weathered biotites generally overlap in heterogeneous samples. The concentrates were examined under binocular and petrographic microscopes, and indices of refraction were measured in oil immersion mounts. The optic axial angles were measured on several hundred flakes of each concentrate by means of an auxiliary microscope and calculated by Mallard's method. These and additional data are given in Table 5.

An X-ray diffractometer and powder cameras were used to determine impurities and to identify recrystallization products in ignited samples, and to measure lattice parameters and intensity ratios of basal reflections (Table 5 and Fig. 4). Weissenberg patterns were obtained on fresh and dehydrated micas (Plate 1) as well as on fresh and weathered portions of a mica flake mounted parallel and perpendicular to the optic axial plane.

Partial chemical analyses of all concentrates were made by X-ray and emission spectroscopy (Table 3), and complete chemical analyses were performed on biotites *43F*, *45F*, and *45W* (Table 1). Water, ferrous and ferric iron, potassium, and radiogenic argon were determined in laboratory oxidized and dehydrated biotites (Table 2).

https://doi.org/10.1346/CCMN.1967.0150139 Published online by Cambridge University Press

TABLE 1.—CHEMICAL ANALYSES OF ORIGINAL BIOTITES

Analysts: S. Abbey, J. L. Bouvier and J. A. Maxwell of the Analytical Chemistry Section, GSC

Weight %	*43F*	*45F*	*45W*
SiO_2	33.80	33.58	32.19
Al_2O_3	19.22	17.69	17.97
TiO_2	2.05	1.27	1.12
Fe_2O_3	3.64	8.49	24.92
FeO	16.63	19.40	2.87
MgO	8.81	4.58	5.14
MnO	0.61	0.65	0.58
Cr_2O_3	0.02	0.04	0.04
NiO	0.02	0.01	0.02
V_2O_5	0.04	0.01	0.02
Li_2O	0.13	0.14	<0.01
K_2O	9.69	9.59	6.73
Na_2O	0.22	0.27	0.26
CaO	0.05	0.04	0.46
BaO	0.05	0.02	0.12
Rb_2O	0.04	0.01	<0.01
H_2O^+	2.92	2.32	4.77
H_2O^-	0.60	0.68	1.68
F	0.45	0.65	0.60
Cl	0.68	0.20	I.S.*
P_2O_5	<0.01	0.07	0.06
S	0.03	I.S.	I.S.
CO_2	0.20	0.12	0.00
Total	99.90	99.83	99.55
Less O=F, Cl	0.34	0.31	0.25
Net total	99.56	99.52	99.30

* I.S. = insufficient sample; minor elements reported in Table 3.

A few fresh and altered mica specimens were studied by means of infrared, differential thermal, and thermogravimetric analyses. Results are given in Figs. 2 and 3. Sample preparation and other procedures used for the infrared analyses have been described by Porteous and Gillieson (1966). Structural formulae were calculated on the basis of forty-four cationic valencies. The unit cell contents of several specimens are given in Table 4.

DISCUSSION

Properties of Fresh Biotites

Chemical.—The fresh biotites contain variable quantities of total iron. Biotites *46F* and *43F* from paragneisses and from a xenolith contain less iron, and biotite *44F* from nepheline syenite pegmatite has more iron than

https://doi.org/10.1346/CCMN.1967.0150139 Published online by Cambridge University Press

TABLE 2.—CHEMICAL ANALYSIS OF HEATED MICAS AND $^{40}Ar/^{40}K$ RATIOS

Weight %	*27A*	*27B*	*27C*	*27D*	*44WC*
Fe_2O_3	11.44	12.11	24.04	20.90	34.83
FeO	11.38	10.87	0.06	2.67	0.08
H_2O	1.76	0.74	0.07	0.08	0.21
F	0.54	0.67	0.52	0.58	
K*	7.76	7.73	7.77	7.77	
$^{40}Ar/^{40}K$	0.1874	0.0923	0.1158	0.0994	
% Radiogenic argon†	98	31	98	99	

Chemical analysis of iron, water and fluorine by S. Abbey and J. L. Bouvier.
* X-ray spectrochemical determination of potassium by Mrs. M. E. Bartlet.
† Radiogenic argon and $^{40}Ar/^{40}K$ ratios determined by the staff of the Isotope Geology Section under the supervision of Dr. R. K. Wanless.

the other biotites. Biotites *27*, *31*, *43F*, and *45F* have lower Si/Al ratios than ideal mica and therefore the negative charge on the tetrahedral layer exceeds two (2.73 to 2.85). The number of trivalent and quadrivalent ions (aluminium, titanium, and ferric iron) in the octahedral layer of these biotites varies from 1.29 to 1.69, and the octahedral occupancy varies from 5.48 (biotite *45F*) to 5.74 (biotite *31 green*). The biotites differ in the quantities of the octahedral aluminium and ferric iron, and in deficiency of the (OH,F)-group. Brown biotite *27* from cordierite schist has the highest octahedral aluminium and the lowest ferric iron content, while green biotites *31* and *45F* from alkalic pegmatites contain the highest proportions of ferric iron. More detailed studies are needed in order to explain the origin of high ferric iron in the fresh biotites from the alkalic rocks. As can be seen from a comparison of bitotite *31 green* and *43F*, deficiency of the (OH,F)-group does not bear any direct relationship to quantity of ferric iron. These biotites contain the same number of ions in the (OH,F)-group, but green biotite *31* has twice as much ferric iron as *43F*.

Thermal behaviour.—Biotites *43F* and *45F* contain considerable quantities (0.6%) of adsorbed water (Fig. 1, bottom left), which is retained after drying and gives a prominent peak in the 3 μ region of the infrared absorption spectrum (Fig. 2, biotite *45F*). Biotite *31 green* gives, after drying, a sharp OH-peak in the 2.75 μ range. The peak of adsorbed water in the 3 μ range was detected in comminuted biotite *27*, but it disappeared after drying (Fig. 2, biotites *27* "*as received*" and *27*). Differential thermal and thermogravimetric analyses of biotite *27* indicated that loss of constitutional water is masked by the process of oxidation (Fig. 3). The total loss of weight recorded on the thermogravimetric balance is less than half of the total water and fluorine contents determined by chemical analysis. A sluggish oxidation reaction culminates at *ca.* 500°C, and is followed by a shallow endothermic peak that ends at *ca.* 1000°C. The biotite recrystallizes to spinel

https://doi.org/10.1346/CCMN.1967.0150139 Published online by Cambridge University Press

https://doi.org/10.1346/CCMN.1967.0150139 Published online by Cambridge University Press

TABLE 3.—TOTAL IRON AND MINOR ELEMENTS IN FRESH AND WEATHERED BIOTITES

Weight %	*31 green*	*31 orange*	*43F*	*44F*	*44W*	*45F*	*45W*	*46F*	*46W*
Emission spectrographic analysis by K. A. Church, J. P. Malone, and W. F. White									
B			0.011			0.013	0.023		
Ba	0.044	0.033	0.045			0.015	0.11		
Ca	0.069	0.38	0.039			0.029	0.33		
Cr	N.D.*	0.022	0.016			0.030	0.027		
Cu	0.006	0.006	0.001			0.003	0.013		
Mg	1.6	2 2	10.			4.3	6.6		
Mn	0.82	0.67	0.75			0.68	0.53		
Ni			0.013			0–011	0.016		
V	0.008	N.D.	0.022			0.006	0.006		
Yb	N.D.	0.003							
Y	N.D.	0.021							
X-ray spectrochemical analysis by Mrs. M. E. Bartlet and G. R. Lachance									
BaO†	0.1		0.09	0.05	0.03	0.06		0.06	0.08
CaO	0.1		0.1	<0.05	0.7	0.05		1.5	1.8
Cl†	0.9		0.68	0.5	0.8	0.2		0.3	0.4
Total Fe as Fe_2O_3	28.6		23.8	35.8	34.4	30.1		20.9	22.3
K_2O	8.3		9.6	9.8	6.6	9.8		7.5	3.2
MnO	0.9		0.6	0.6	0.6	0.6		0.3	0.4
TiO_2	1.7		2.4	0.9	1.0	1.4		1.2	1.2
CuO ppm	200		<50	<50	<50	<50		<50	<50
NiO ppm	90		130	N.D.	90	90		260	290
Rb ppm	650		400	370	300	330		520	320
Sr ppm	10		20	<20	20	30		30	70
Zn ppm	1800		2640	2970	2510	2480		3020	3800

* N.D. = not detected.

† Spectrochemical determinations not significant because of low intensities.

https://doi.org/10.1346/CCMN.1967.0150139 Published online by Cambridge University Press

TABLE 4.—UNIT CELL CONTENTS (Calculations based on forty-four cationic valencies)

Layer	Conversion factor	*31 green** 9.42	*43F* 9.23	*45F* 9.42	*45W* 9.34	*44WC* 8.61	*27** original 9.18	*27A* 8.99	*27B* 8.97	*27C* 8.70	*27D* 8.64
Octahedral	Al	0.26	0.658	0.54	0.279	—	0.861	0.672	0.65	0.398	0.332
	Ti	0.18	0.237	0.15	0.13	0.05	0.361	0.356	0.353	0.342	0.339
	Fe'''	0.85	0.420	1.00	2.914	3.78	0.214	1.286	1.359	2.62	2.503
	Fe''	2.93	2.136	2.54	0.372	0.01	2.66	1.411	1.356	0.008	0.321
	Mg	1.40	2.017	1.07	1.191	1.00	1.41	1.384	1.381	1.340	1.330
	Mn	0.12	0.079	0.090	0.076	0.08					
	Cr, Ni, V		0.006	0.006	0.008		0.020	0.018	0.018	0.017	0.017
	Li		0.08	0.088							
	Occupancy	5.74	5.633	5.48	4.972	4.92	5.52	5.13	5.13	4.73	4.84
	Charge (+)	0.91	0.82	0.73	1.34	1.72	0.80	0.96	0.99	1.18	1.21
Tetrah.	Si	5.15	5.197	5.27	5.005	4.89	5.26	5.15	5.13	4.98	4.94
	Al	2.85	2.803	2.73	2.995	3.04	2.74	2.85	2.87	3.02	3.06
	Ti					0.07					
	Oxygen	20.28	20.28	20.60	19.38	21.75	20.06	21.00	21.47	21.85	21.83
OH group	Oxygen −20	0.28	0.28	0.60	(−0.62)	1.75	0.06	1.00	1.47	1.85	1.83
	(OH)	3.16	2.99	2.42	4.94	0.20	3.65	1.76	0.74	0.06	0.08
	F	0.27	0.27	0.32	0.30	0.30	0.25	0.24	0.32	0.24	0.26
	Cl		0.18	0.06							
	Occupancy	3.71	3.72	3.40	5.24	2.25	3.96	3.00	2.53	2.15	2.19
Interlayer	Ca	0.003	0.008		0.077		0.046	0.045	0.045	0.043	0.043
	Ba	0.001	0.003	0.001	0.007		0.008	0.008	0.008	0.008	0.008
	Na	0.09	0.065	0.082	0.078	0.07					
	K	1.86	1.900	1.915	1.335	1.23	1.84	1.80	1.79	1.74	1.73
	Rb		0.004	0.001			0.006	0.006	0.006	0.006	0.006

* *Biotite 31 green* and *27*: data taken from Rimsaite (1964) p. 171, table 3. Dehydrated biotites were calculated using chemical analyses of the original biotites and actually determined values of ferric and ferrous iron, water and fluorine (taken from Table 2).

TABLE 5.—COMPARISON OF PHYSICAL PROPERTIES OF FRESH, WEATHERED, AND DEHYDRATED BIOTITES

Specimen no.	Specific gravity	Specific magnetic susceptibility amperes/α*	Optical properties: Colour after Ridgway (1912)	γ	β	α	γ−α	2V°	X-ray diffraction analysis: Chlorite / Biotite	$I_{(004)}/I_{(005)}$	$d_{(001)}$	$d_{(010)}$	Structural modification polymorph†
		0.24	XVII Courage Green	1.660									
31 green	3.20 3.12	0.22 0.21	XXXII Light Fluorite Green	1.650	1.650	1.596	0.054	0–6	N.D.‡	2.07	10.06	9.24	1Md
31 orange			γ: II Orange Chrome	1.740	1.740	1.630	0.110	24	Chlorite	1.45	10.07	9.21	1Md
			β: XVII Courage Green	1.720	1.720	1.620	0.100		trace				
		0.40		1.654									
43F	3.10	0.33 0.25	IV Orange Citrine to Medal Bronze	1.644	1.642 1.638	1.590	0.054	2–6	N.D.	1.34	10.06	9.25	2M
		0.30	γ: XIX Zinc Green										
44F	3.28 3.05	0.28 0.25	β: VI Peacock Green	1.676	1.674	1.614	0.060	0–8	N.D.	2.45	10.07	9.28	1M
			γ: III Cadmium Orange	1.83			0.200						
44FC			β: Citrine	1.82	1.81	1.630	0.190	45	N.D.	2.41	9.97	9.25	
			Red specks: IV Orange Rufous										
		0.40	γ: III Xanthine Orange										
44W	2.98 2.95	0.30 0.25	β: III Light Orange Yellow	1.75	1.73	1.573	0.177	16–23	N.D.	1.50	10.08	9.22	1Md
				1.83									
44WC			γ: II Salmon Orange	1.82	1.82	1.616	0.214	26–45	N.D.	2.11	9.96	9.18	
			β: IV Apricot Yellow										
		0.30	VI Peacock Green	1.660	1.658	1.608	0.054						
45F	3.20 3.10	0.27 0.25	XVIII Dark Yellowish Green XVI Dull Citrine	1.654	1.650	1.600	0.052	0–24	N.D.	1.94	10.07	9.27	3T and 1M
		0.44	γ: III Salmon Orange										
45W	3.09 2.93	0.40 0.35	β: III Orange Buff	1.760	1.740	1.610 1.576 tr	0.146	16–34	N.D.	1.25	10.07	9.27	3T and 1M

https://doi.org/10.1346/CCMN.1967.0150139 Published online by Cambridge University Press

https://doi.org/10.1346/CCMN.1967.0150139 Published online by Cambridge University Press

46F	3.05 2.90	0.40 0.35 0.25	IV Citrine to Warbler Green	1.636 var.	1.634	1.588	0.048	0–8	Chlorate trace	0.94	10.07	9.24	1M
46FC			γ: I Scarlet β: II Orange Chrome Interference Colour Flame-Red	1.728 1.720	1.720 1.716	1.600	0.128	22–45	N.D.	0.97	9.98	9.20	
46W	2.70 2.60	0.50 0.43 0.35	γ: II Orange Rufous β: III Capucine Yellow	1.630 1.620	1.628 1.618	1.568 1.564	0.062 0.056	9–26	2.5	0.87	10.06	9.21	1Md
46WC			γ: I Scarlet to II Salmon Orange β: II Orange Chrome	1.728 Rare: 1.670	1.720 1.660	1.598 1.594	0.130 0.076	22–34	N.D.	0.99	9.99	9.19	
27	3.10 3.08	0.33 0.27 0.24	II Burnt Sienna III Capucine Buff IV Baryte Yellow	1.648 1.644	1.646 1.642	1.596 1.590	0.052 0.054	6–8 8–15 29plHalo	0.02	1.35	10.04	9.24	1M
27A		0.40 0.35 0.30	IV Orange Citrine XXXI Lime Green; along fractures: III Mars Yellow	1.714 Edge: 1.72	1.708	1.600	0.114	8–43	N.D.	1.13	9.95	9.17	1M
27B		0.45 0.35 0.25	IV Citrine II Mars Orange to Opaque	1.696 1.674	1.680 1.668	1.604 1.600	0.092 0.074	12–34	N.D.	1.41	10.01	9.18	1M
27C		0.50 0.45 0.35	II English Red γ: III Cadmium Orange β: III Light Orange Yellow	1.748 1.730	1.720 1.710	1.622 1.620	0.126 0.110	8–43	N.D.	1.12	9.95	9.17	1M
27D		0.45 0.35 0.25	γ: III Xanthine Orange β: IV Aniline Yellow	1.748 1.740	1.735 1.730	1.622 1.614	0.128 0.126	43–45	N.D.	1.14	9.96	9.17	1M

* Magnetic susceptibility measured by means of "Frantz" isodynamic separator, reported as minimum and maximum currents required to commence separation and as a critical current (underlined), using a constant vertical slope = 30° and transversal slope = 10°.
† Mica polymorphs: 3T, 2M, 1M, 1Md according to Smith and Yoder (1956).
‡ N.D. = chlorite not detected.

at *ca.* 1170°C. Results of thermogravimetric and differential thermal analyses of biotite *46F* are similar to those of *27*, but the endothermic reaction is more prominent at 750°C, and final dehydration and recrystallization take place at *ca.* 1200°C. The biotites heated in argon lose water and recrystallize at a lower temperature than the biotites heated in air.

Physical and optical.—The fresh micas containing a high proportion of ferric iron are green (*45F*, *31 green*), whereas fresh micas containing little ferric iron are brown (*43F*) and reddish-brown (*27*). Indices of refraction, birefringence, specific gravity, and specific magnetic susceptibility increase with increasing iron content (Table 5).

Structural.—The micas show strong basal reflections on X-ray diffractometer charts (Fig. 4). Two of the biotites, *27* and *46F*, show weak traces of chlorite reflections (second-order basal reflection, 7 Å) as a result of slight alteration along fractures and edges. Intensity ratios of basal reflections, $I_{(004)}/I_{(005)}$, increase with increasing iron content, but spacings $d_{(001)}$ and $d_{(010)}$ do not show any definite relation to chemical composition of the biotites. Most of the flakes of these biotites X-rayed using the Weissenberg method showed single-layer monoclinic structures; however, brown biotite *43F* shows two-layer monoclinic, and one flake of biotite *45* shows a three-layer rhombohedral pattern (Plate 1).

Properties of Intermediate Biotites

1. *Weathered Biotites: 44W, 45W, 46W, 31 orange*

Chemical.—The weathered biotites show considerable differences in iron content (Tables 1 and 3), specimen *46W* containing least and biotite *44W* most iron. Alumina, fluorine, iron, titanium, manganese, nickel, sodium, vanadium, and zinc remain almost the same in the weathered biotites as in their fresh parent micas. The weathered micas, however, lose 30% to 60% potassium, some lithium and rubidium, about 3% silica, and gain water, calcium, magnesium and possibly barium, chlorine, strontium, ytterbium, and yttrium. The apparent gain of calcium, magnesium, and other elements is probably a result of surface contamination by circulating aqueous solutions through the (001) fractures of the weathered biotites. The most significant change, however, is in the oxidation state of iron. The ratio of ferric iron to ferrous iron changes from 0.35 in fresh biotite *45F* to 6.7 in weathered biotite *45W*. The tetrahedral layer of weathered biotite *45W* carries three negative charges. The octahedral layer, composed predominantly of trivalent ions (3.2) carries a positive charge (1.3) and has 4.97 occupied positions which place it intermediate between the dioctahedral and trioctahedral micas. The weathered biotite differs from ideal trioctahedral mica by having a higher content of tetrahedral aluminium (3 instead of 2), lower octahedral occupancy (5 instead of 6), higher number of trivalent ions in the octahedral layer (3.2), lower interlayer content (1.5 instead of 2), and by an increase of the (OH,F)-group components (5.2 instead of 4).

https://doi.org/10.1346/CCMN.1967.0150139 Published online by Cambridge University Press

The chemical differences between the fresh and weathered biotites *45F* and *45W* are very similar to those discussed by Eskola (1949), and, in part, to the results obtained by Walker (1949). The main difference between the observations by Walker and those of Eskola and the present writer is that, according to Walker, biotite loses about one-half of its magnesium, whereas the present data and the analysis reported by Eskola show that magnesium remains in the weathered biotite.

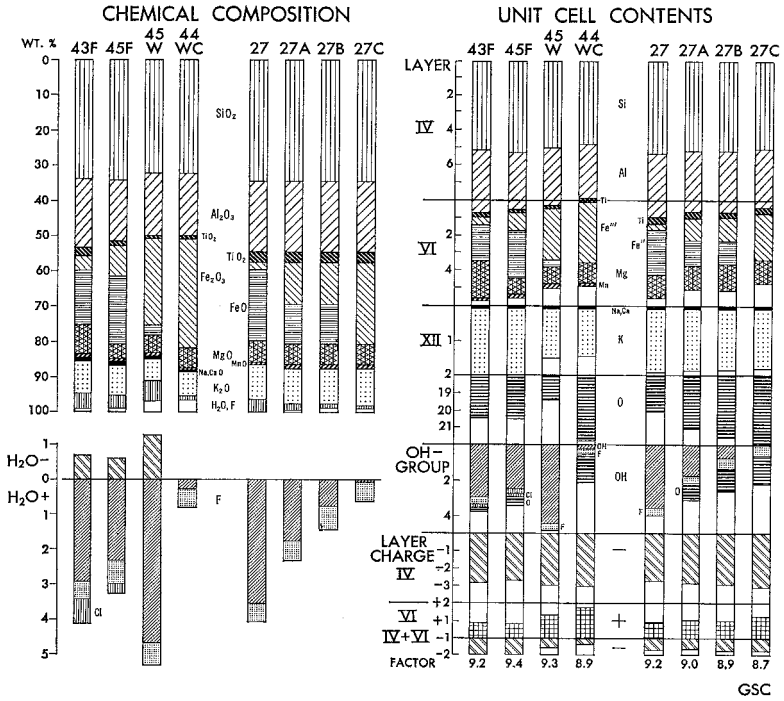


FIG. 1. Graphical presentation of the chemical composition of fresh, weathered and dehydrated biotites (1–8 columns, left), and unit cell contents and layer charges of the same biotites (9–16 columns, right). Lower columns, left, present the quantities of adsorbed water (H_2O^-), constitutional water (H_2O^+), fluorine and chlorine.

Thermal behaviour.—The weathered biotite has a very high quantity of adsorbed water (Fig. 1), which remains after conventional re-drying procedure, as indicated by very prominent peaks in the 3 μ range of the infrared spectra of biotites *45W* and *45W* "redried" (Fig. 2). Differential thermal and thermogravimetric analyses of weathered specimen *46W* indicate that the specimen contains almost 13% of total water, most of which is lost at two steps: below 200°C and 400°C. The final dehydration takes place at *ca.* 1000°C

https://doi.org/10.1346/CCMN.1967.0150139 Published online by Cambridge University Press

and 1200°C. Recrystallization takes place at 900°C, at a lower temperature than its parent biotite *46F*.

Physical and optical.—In specimens too small for chemical analysis, physical properties are the only means of identifying the weathering products. The fresh and altered micas show striking differences in optical properties. During the process of natural oxidation, the colour changes from bright green and olive-brown to bright orange-yellow. The oxidized flakes exhibit a distinct

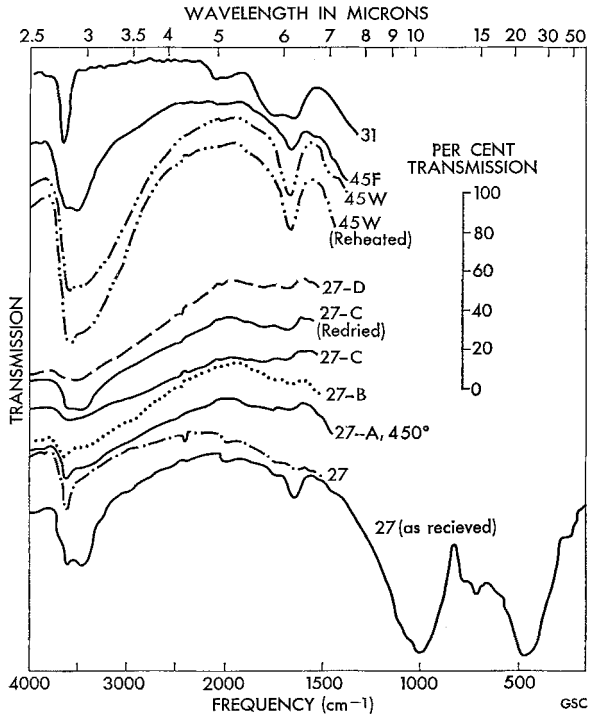


FIG. 2. Infrared absorption spectra of bonded hydroxyl (2.75 μ range) and of adsorbed water (3 μ range) in fresh, weathered and dehydrated biotites. Specimens *45W* and *27C* apparently retain some adsorbed water after redrying. Infrared analyses by P. E. Porteous and A. H. Gillieson.

γ–β pleochroism. In heterogeneous flakes the contact between green (fresh) and yellow (weathered) portions is either sharp, separated by a fracture, or gradual. In some crystals the yellow and green flakes are interleaved at the contact. The yellow weathered portions are usually blistered and exhibit accordion-like swelling, (001) splitting, and polygonal cracks on the (001) cleavage faces (Rimsaite, 1963, pl. III-5). On traversing from fresh to altered portions of a heterogeneous flake, the optic angle 2V gradually changes from 0° to 25°. Indices of refraction, birefringence, and optic axial angles increase

https://doi.org/10.1346/CCMN.1967.0150139 Published online by Cambridge University Press

with increasing quantities of ferric iron, and are higher in weathered biotites than in the parent fresh biotites. Weathering product *46W*, however, has lower indices of refraction than fresh biotite *46F* (Table 1). For the purpose of distinction, weathered biotite having higher indices of refraction than fresh biotite is referred to as type 1, whereas the weathering product having lower indices of refraction than the parent mica is called type 2. Specific gravity and specific magnetic susceptibility are lower in all weathered biotites than in the fresh biotites. These properties are very useful in choosing proper concentration procedures.

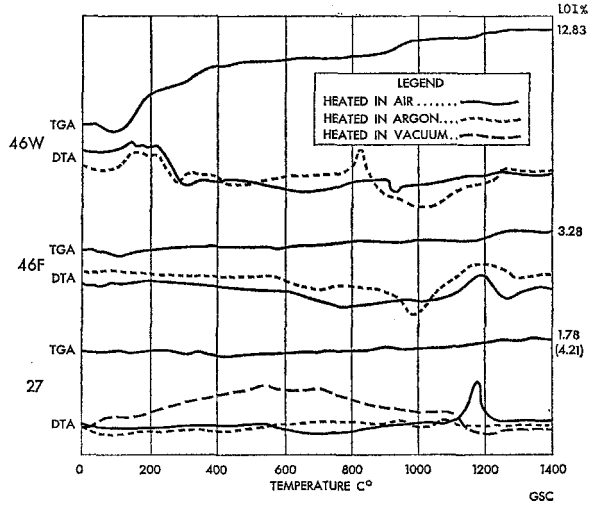


FIG. 3. Differential thermal and thermogravimetric analyses of fresh and weathered biotites; heating rate 12°C/min and 6°C/min, respectively. Analyst R. H. Lake. L.O.I. is loss of weight recorded, figure in brackets indicates total weight of water and fluorine determined by chemical analysis.

Structural.—All the weathered biotites of type 1 retain the basal spacing of mica. The type 2 weathering product (*46W*), however, shows strong basal reflections of chlorite–vermiculite in addition to the reflections of mica (Fig. 4). Biotite *31 orange* shows a weak second-order basal reflection of chlorite (7 Å). Basal reflections of weathered biotites *44W*, *45W*, and *31 orange* are broader and much weaker than those of the fresh parent biotites; the spacings $d_{(001)}$ and $d_{(010)}$, however, remain almost the same (Fig. 4 and Table 5). Intensity ratios $I_{(004)}/I_{(005)}$ in the weathered biotites are lower than in the fresh parent biotites partly as a result of general decreasing intensities and broadening of higher order basal reflections of the weathered biotites (Fig. 4).

X-ray diffraction Weissenberg photographs of fresh and weathered portions of the same flake show that the weathered biotites retain the structural

https://doi.org/10.1346/CCMN.1967.0150139 Published online by Cambridge University Press

modification of the parent mica. Superimposed Weissenberg X-ray diffraction photographs (Plate 1) of fresh and weathered three-layer rhombohedral biotites *45F* and *45W* show that the reflections of altered biotite *45W* are more diffuse than those of *45F*, and that the patterns differ in the intensities of the basal reflections. The change in the intensities of the basal reflections

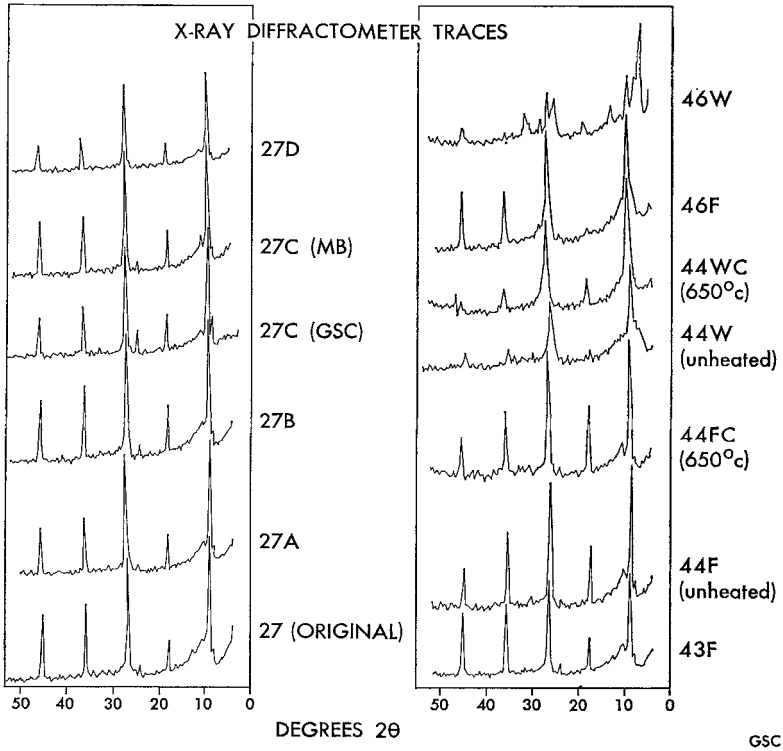


FIG. 4. Basal reflections of fresh, weathered and heated biotites. Ni filtered Cu radiation, 45 kV, 16 mA. Weathered unheated biotite *44W* shows weaker basal reflections than the same heated biotite *44WC* and the parent biotite *44F*. Weathering product *46W* shows prominent chlorite–vermiculite reflections, in addition to basal reflections of mica. Basal spacings decrease in heated biotites.

in the oxidized biotite *45W* is probably a result of rearrangement of ions, similar to that observed by Eberhart (1963) in heated muscovites. Although the Weissenberg patterns are similar and apparently indicate rhombohedral symmetry, the fresh mica is uniaxial and the altered portion is biaxial with 2V reaching 30°, perhaps as a result of an internal strain in the crystal. The diffuse scattering is attributed in part to structural disorder and to the fractured-split nature of the altered flakes which may cause them to diffract X-rays like composite crystals.

https://doi.org/10.1346/CCMN.1967.0150139 Published online by Cambridge University Press

2. *Laboratory Heated Biotites 44 and 46*

Chemical.—Almost all of the iron contained in heated weathered biotite *44WC* has been oxidized, and most of its water and hydroxyl has been driven off. Total iron remains the same in the unheated and heated biotites. The octahedral layer of the heated biotite is composed mainly of trivalent ions (3.8) and its occupancy is almost 5 (4.92). The main difference between the heated and unheated biotites is in their (OH,F)-group contents. In the heated biotite *44WC* the (OH,F)-group is deficient and it is composed mainly of oxygen (Fig. 1 and Table 4).

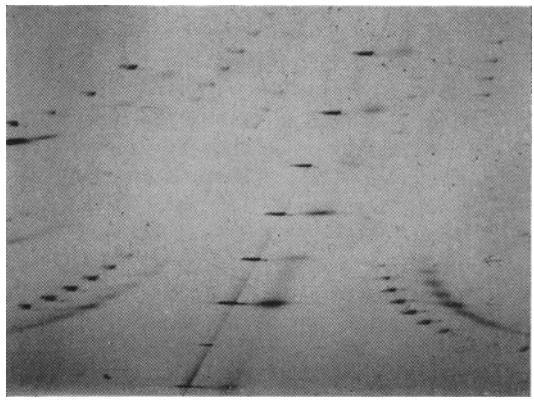


PLATE 1. Superimposed single-crystal Weissenberg *a*-axis 0-layer patterns. Mn filtered Fe radiation. X-ray analyst Miss C. M. Hunt. Green biotite *45F* (left) and altered orange-yellow portion of the same flake *45W* (right, diffuse scattering) both show reflections of three-layer rhombohedral biotite. Basal reflections of the altered biotite exhibit more prominent intensity variations than do those of fresh biotite.

Physical and optical.—The heated biotites are fractured, split along (001) cleavage planes, blistered, and very brittle. The colour of fresh biotite changes on heating from brown and green to orange-red and that of weathered biotites from orange-yellow to bright orange-red. The basal cleavage flakes of all the heated biotites are pleochroic with γ dark orange-red and β pale yellow, and exhibit bright red and orange interference colours. The refractive indices, birefringence, and the optic axial angles increase in all heated biotites. Optical properties of heated biotite *44FC* (fresh) and *44WC* (weathered) are very similar (Table 5). As can be seen from Table 3, potassium is depleted in mica *44W* whereas ferric iron is about the same in both heated micas. Thus, the effect of potassium (6.6% in *44W* and 9.8% in *44F*) on the magnitude of the index of refraction is negligible in comparison to ferric iron. Although the physical properties of unheated samples *46W* and *46F* are quite different, after heating they are almost the same (Table 5, *46FC*, and *46WC*).

https://doi.org/10.1346/CCMN.1967.0150139 Published online by Cambridge University Press

Structural.—The basal mica reflections become stronger and sharper on heating weathered biotites and the chlorite and chlorite–vermiculite reflections disappear. The intensity ratios $I_{(004)}/I_{(005)}$ of the heated weathered biotites are almost as high as in unheated and heated fresh biotites (Table 5). The spacings $d_{(001)}$ and $d_{(010)}$ decrease in all heated biotites.

3. *Laboratory Heated Biotite 27*

Chemical.—The potassium content of biotite *27* remains the same on heating, while the quantity of oxidized iron, dehydration, loss of radiogenic argon and adsorption of the atmospheric argon vary according to the experimental conditions (Table 2 and Fig. 1). The octahedral layer of all heated biotites *27A–D* contains about five occupied positions (4.84 to 5.13) and carries a positive charge from 0.96 to 1.21. The octahedral occupancy decreases and the positive charge increases with increasing quantities of ferric iron. The number of trivalent elements increases from 1 in unheated biotite *27* to 1.8 in *27A* and 3 in *27C*. The ratio of ferric to ferrous iron increases from 0.08 in original biotite *27* to 0.9 in *27A*, 1 in *27B*, 328 in *27C*, and to 8 in *27D*. The occupancy of the (OH,F)-group decreases with increasing quantity of ferric iron, and oxygen replaces the hydroxyl. The heated biotites differ from the ideal dioctahedral and trioctahedral micas in the number of ions in the octahedral positions (5 in the heated, 4 or 6 in the ideal micas) and in the number of anions.

These differences will be discussed in more detail in a separate paper.

Thermal behaviour.—A comparison of infrared absorption spectra (Fig. 2) shows that although the hydroxyl and water peaks in the 3 μ range decrease in heated and dried biotites, the dehydrated specimens are very susceptible to adsorption of atmospheric moisture (Fig. 2, biotite *27C* "redried"). A chemical analysis performed on the dehydrated biotite removed from a desiccator indicated that in 1 hr the biotite adsorbed 2% water.

Physical and optical.—Comparison of optical properties (Table 5) of biotite *27* and its oxidation and dehydration products *27A–D* indicates: (1) that some flakes, particularly those of *27A* and *27B*, are optically heterogeneous, thus not uniformly dehydrated, and (2) that the index of refraction does not increase uniformly with temperature but is a factor of the atmospheric conditions in which the experiment was carried out. The most homogeneous biotite is *27C*. It has the highest indices of refraction and the highest birefringence. It is interesting to point out that by heating a homogeneous mica under different atmospheric conditions, it can be altered to different heterogeneous micas. This observation is important in connection with the interpretation of the origin of similar heterogeneous flakes that are very common in igneous and metamorphic rocks and vary in colour from green to orange-red and opaque.

The magnetic susceptibility of heated biotites *27A–D* is slightly lower than that of the original biotite *27* (Table 5).

https://doi.org/10.1346/CCMN.1967.0150139 Published online by Cambridge University Press

Structural.—X-ray diffractometer traces of unheated and heated biotites *27* and *27A–D* are similar, but the spacings $d_{(001)}$ and $d_{(010)}$ of the heated biotites show distinct contraction which is correlative with the proportion of oxidized iron.

All unheated and heated biotites *27* and *27A–D* have a single-layer monoclinic structure and give similar Weissenberg patterns.

Retention of argon.—As can be seen from Table 2, the potassium content remains the same in heated biotites *27A–D*, while the ratio of radiogenic argon to potassium shows considerable variations. The highest loss of argon is from biotite *27B* and it is interesting to point out that this biotite contains more hydroxyl than *27C* and *27D*, indicating that the relationship between the loss of argon and loss of water does not conform to the direct relationship between the loss of argon and loss of water observed by Amirkhanoff and associates (1961) for muscovite. Biotite *27B*, heated in argon, contains proportionately more atmospheric argon than biotites *27A*, *C* and *D* (Table 2). This confirms results published by Karpinskaya and associates (1961) who showed that argon can be instilled (introduced) into micas by heating them in an argon atmosphere.

SUMMARY

Biotite intermediate between dioctahedral and trioctahedral micas occurs in nature and is a weathering product of iron-rich biotites. A similar biotite can also be produced by heating biotite that contains high ferrous iron. The characteristic chemical, physical and structural properties of these biotites are:

1. *Fresh biotites* vary in iron content and in deficiency of the (OH,F)-group. All the biotites contain more than two aluminium ions in the tetrahedral layer, which carries a negative charge varying from 2.73 to 2.85. The octahedral occupancy varies from 5.48 to 5.74, the positive charge from 0.73 to 0.91, and the ratio of ferric to ferrous iron from 0.08 to 0.4. The interlayer contains between 1.95 and 1.99 alkali and calcium ions.

2. *Weathered biotites.* Two types of weathering products are distinguished: (1) weathered biotites that retain the structure of mica, and (2) altered flakes consisting of biotite–chlorite–vermiculite intergrowths. Weathered biotites that still retain the structure of mica retain most of the major constituents of the fresh biotites, while losing potassium and some rubidium, and gaining water. The octahedral occupancy of the weathered biotite is close to five and the ratio of ferric iron to ferrous iron increases to 8. The number of alkali metals in the interlayer decreases to 1.5, and the number of the (OH,F)-group components exceeds 4.

Physical properties of weathering products vary depending on the weathering type: in weathered biotite that retains the structure of mica (type 1) indices of refraction are higher than in the parent biotite, whereas in the weathered flakes that consist of biotite–chlorite–vermiculite intergrowths (type 2) the refractive indices are lower than in the parent fresh biotite.

https://doi.org/10.1346/CCMN.1967.0150139 Published online by Cambridge University Press

3. *Heated biotites.*—The octahedral occupancy in all heated biotites is close to five, the positive charge varies from 0.9 to 1.6, and the ratio of ferric iron to ferrous iron varies from 0.9 to 330. Alkali metals and the occupancy of the interlayer vary from 1.3 in heated weathered biotite to 1.9 in heated fresh biotite; and the contents of the (OH,F)-group vary from 2.15 to 3.00, depending on the degree of dehydration and quantities of original fluorine. Hydroxyl is replaced by oxygen. The indices of refraction and optic axial angles increase with increasing ferric iron and with decreasing hydroxyl. Biotite heated in an argon atmosphere is only partly oxidized and dehydrated but apparently loses more radiogenic argon than entirely dehydrated and oxidized biotites heated in air and in vacuum. The weathered and heated biotites retain the structure of the parent micas; single-layer and two-layer monoclinic, and three-layer rhombohedral patterns were obtained on fresh and altered portions of single biotite flakes.

Results of the present study contribute to a better understanding of chemical and physical changes taking place in iron-rich biotite as a result of weathering in its parent rock. It is shown that before reaching a clastic sediment, biotite may be already oxidized, depleted of one half of its potassium and partly altered to chlorite–vermiculite. It is believed that this comparative data on the chemical and physical properties of fresh original, weathered and dehydrated biotite will be useful in synthetic studies and studies of detrital biotites in soils and other sediments.

ACKNOWLEDGMENTS

The writer wishes to thank Mr. L. F. McDonnell, Area Manager, Blue Mountain Plant of the International Minerals and Chemical Corporation (Canada) Limited, for the permission to collect specimens in the nepheline deposit and his helpful suggestions in the field. Miss Donna Daniels assisted in the preparation of the drawings, Mr. R. N. Delabio performed the X-ray diffraction analyses, and Mr. R. H. Lake of the Mines Branch, Department of Energy, Mines and Resources, prepared the dehydrated specimens and carried out the differential thermal and thermogravimetric analyses. Their help and the assistance of all who contributed to experimental studies is gratefully acknowledged. The writer is indebted to Dr. R. J. Traill and Dr. F. Aumento for discussions and constructive criticism of the manuscript.

REFERENCES

AMIRKHANOFF, K. I., BRANDT, S. B., and BARTINSKY, E. N. (1961) Radiogenic argon in minerals and its migration: *Ann. N.Y. Acad. Sci.* **91** (Art. 2), 235–75.

EBERHART, J. P. (1963) Étude des transformations du mica muscovite par chauffage entre 700 et 1200°C: *Bull. Soc. Franç. Minéral.* **86**, 213–51.

ESKOLA, P. (1936) On the disintegration of rapakivi: *Bull. Commiss. Geol. Finlande* **92**, 96–105.

ESKOLA, P. (1949) The mica of the Moro: *Bull. Commiss. Geol. Finlande* **114**, 113–16.

https://doi.org/10.1346/CCMN.1967.0150139 Published online by Cambridge University Press

GOLDSCHMIDT, V. M., and JOHNSON, M. (1922) Glimmermineralernes betydning som kalikilde for planterne: *Norges geol. Unders.* **108**, 89.

GRANT, W. H. (1964) Chemical weathering of biotite–plagioclase gneiss: *Clays and Clay Minerals*, Proc. 12th Conf., Pergamon Press, New York, 455–63.

KARPINSKAYA, T. B., OSTROVSKYI, I. A., and SHANIN, L. L. (1961) Artificial instillation of argon into mica at high pressures and temperatures: *Izvestya* (*Newsletter*) *Acad. Sci. U.S.S.R.*, Geol. Series, No. 8.

PORTEOUS, P. E., and GILLIESON, A. H. (1966) Feasibility of quantitative determination of bonded hydroxyl in biotites by infrared spectroscopy: *Dept. Mines Tech. Surveys, Mines Branch, Min. Sci. Div. Int. Rept.* MS 66–29, 4 pp.

RIDGWAY, R. (1912) Color standards and nomenclature: Washington, D.C. (published by the author).

RIMSAITE, J. Y. H. (1963) Studies of rock-forming micas: *Bull. Geol. Survey, Canada*, **149** (in press).

RIMSAITE, J. (1964) On micas from magmatic and metamorphic rocks: *Beitr. Min. Petrogr.* **10**, 152–88.

SMITH, J. V., and YODER, H. S. (1956) Experimental and theoretical study of the mica polymorphs: *Min. Mag.* **31**, 209–34.

TSVETKOV, A. I., and VALYASHIKHINA, E. P. (1956) Data on thermal studies of minerals: III Micas: *Trans. Inst. Geol., Mining, Mineral., Geochem.*, Ed. 4, Moscow, Acad. Sci. U.S.S.R.

WALKER, G. F. (1949) The decomposition of biotite in the soil: *Min. Mag.* **28**, 693–703.

https://doi.org/10.1346/CCMN.1967.0150139 Published online by Cambridge University Press